Supporting Information

Unraveling the Atomic Structure of Bulk Binary Ga-Te Glasses with Surprising Nanotectonic Features for Phase-Change Memory Applications

Maria Bokova, Andrey Tverjanovich, Chris J. Benmore, Daniele Fontanari, Anton Sokolov, Maxim Khomenko, Mohammad Kassem, Ilya Ozheredov, and Eugene Bychkov*

* Email: Eugene.Bychkov@univ-littoral.fr

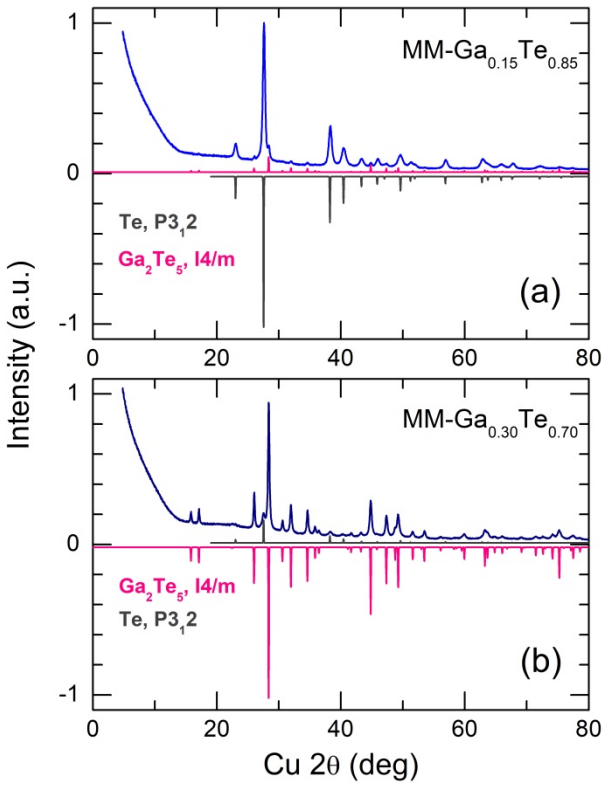

Figure S1. Diffraction pattern of (a) MM-$Ga_{0.15}Te_{0.85}$ and (b) MM-$Ga_{0.30}Te_{0.70}$, prepared by mechanical milling (MM). The main crystalline phase in case of MM-$Ga_{0.15}Te_{0.85}$ is trigonal tellurium, space group $P3_12$.[S1] Tetragonal Ga_2Te_5, $I4/m$,[S2,S3] appears to be the major crystalline species in MM-$Ga_{0.30}Te_{0.70}$.

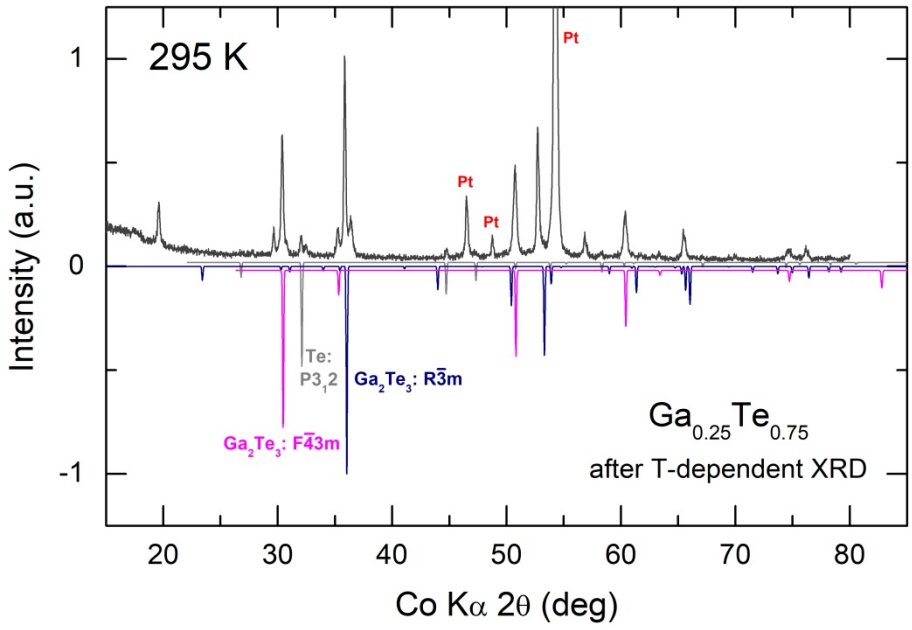

Figure S2. Diffraction patterns of $Ga_{0.25}Te_{0.75}$ sample after *in situ* diffraction measurements as a function of temperature and related crystalline references: cubic Ga_2Te_3,[S4] high-pressure rhombohedral Ga_2Te_3,[S5] and trigonal tellurium.[S1]

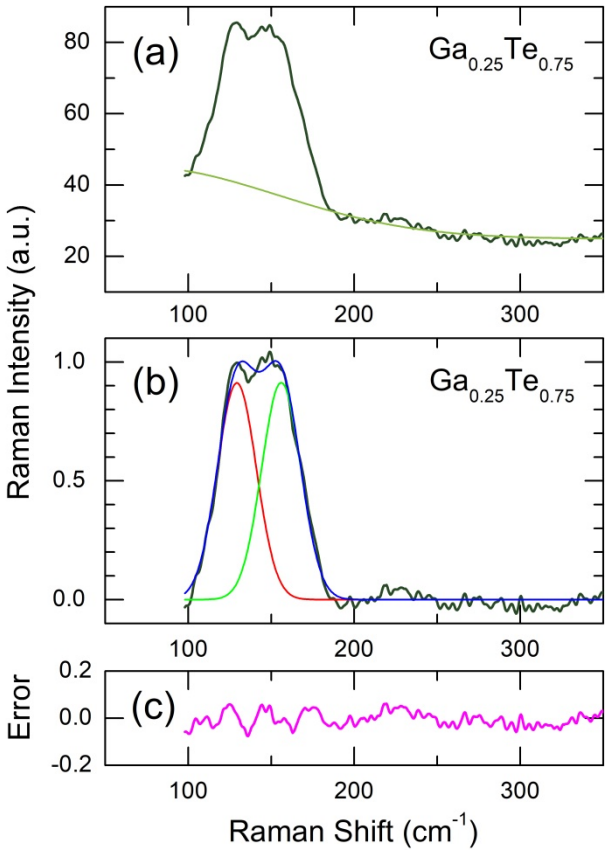

Figure S3. (a) Raw Raman data for bulk glassy $Ga_{0.25}Te_{0.75}$ before baseline subtraction, (b) a two-peak Gaussian fitting of the baseline subtracted and normalized Raman spectrum for $Ga_{0.25}Te_{0.75}$, and (c) difference between experimental and deconvoluted spectra.

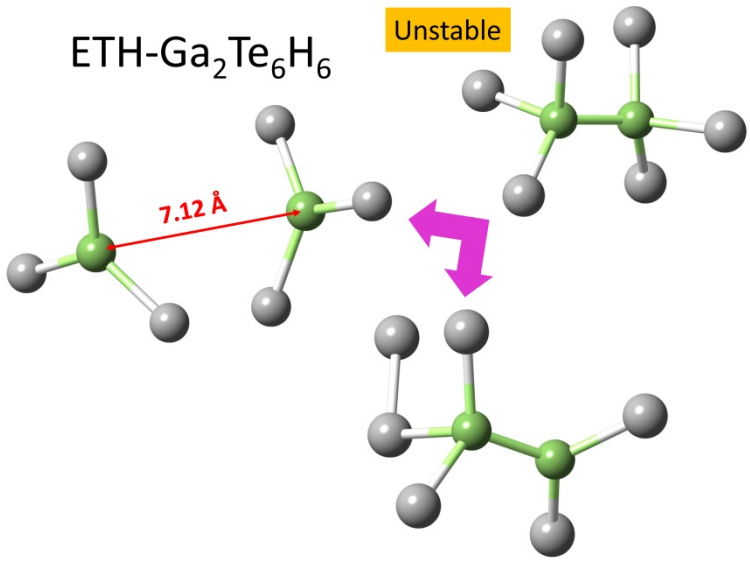

Figure S4. Structural evolution of ETH-$Ga_2Te_6H_6$ cluster during DFT optimization at 0 K. The first scenario consists in a complete separation of the ETH-$Ga_2Te_6H_6$ cluster into two $GaTe_3H_3$ units of approximate D_{3h} geometry distant of 7.12 Å. In the second scenario, a tellurium species moves from one gallium toward the other one forming a Te-Te pair. The terminal hydrogen atoms are not shown.

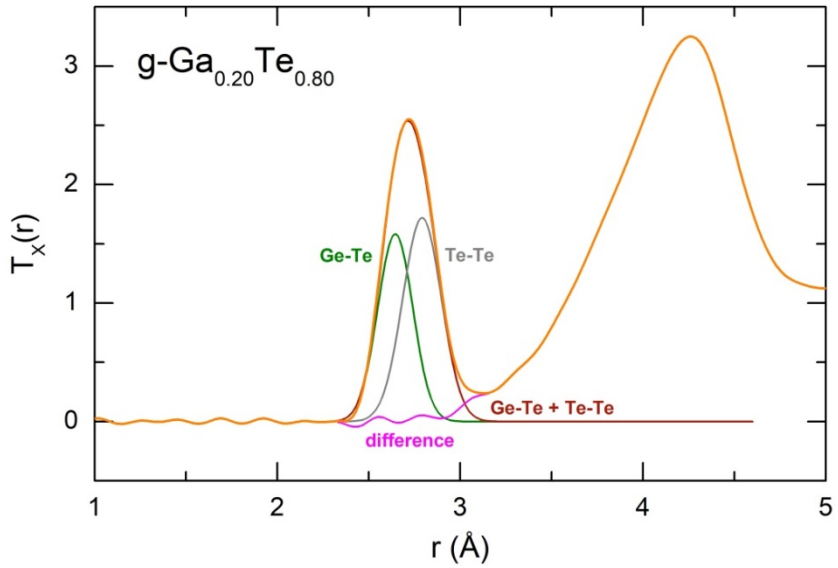

Figure S5. Gaussian fitting of the nearest neighbor peak of the X-ray total correlation function $T_X(r)$ for glassy $Ga_{0.2}Te_{0.8}$: Ge-Te and Te-Te correlations are shown by the green and gray solid lines, respectively, the difference between experimental and deconvoluted data is drawn as the solid magenta line.

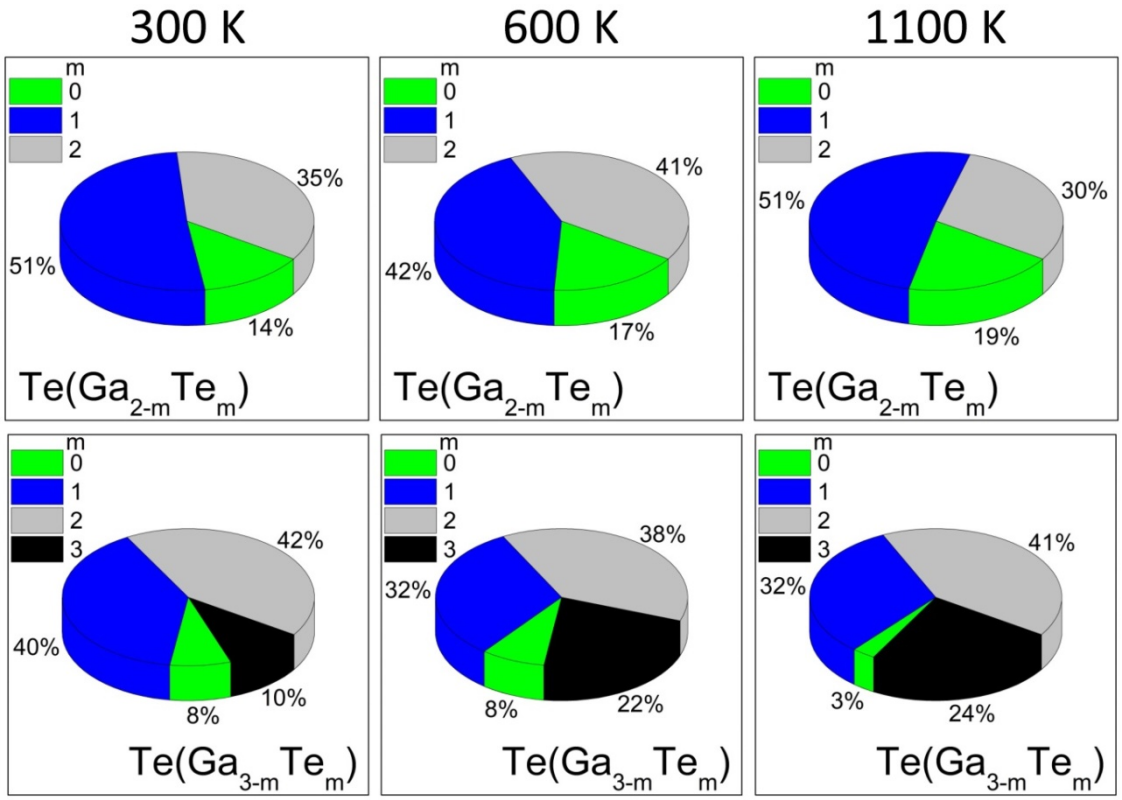

Figure S6. Nearest neighbor distributions around two-fold and trigonal Te species at 300, 600 and 1100 K (enlarged insets to Figure 12).

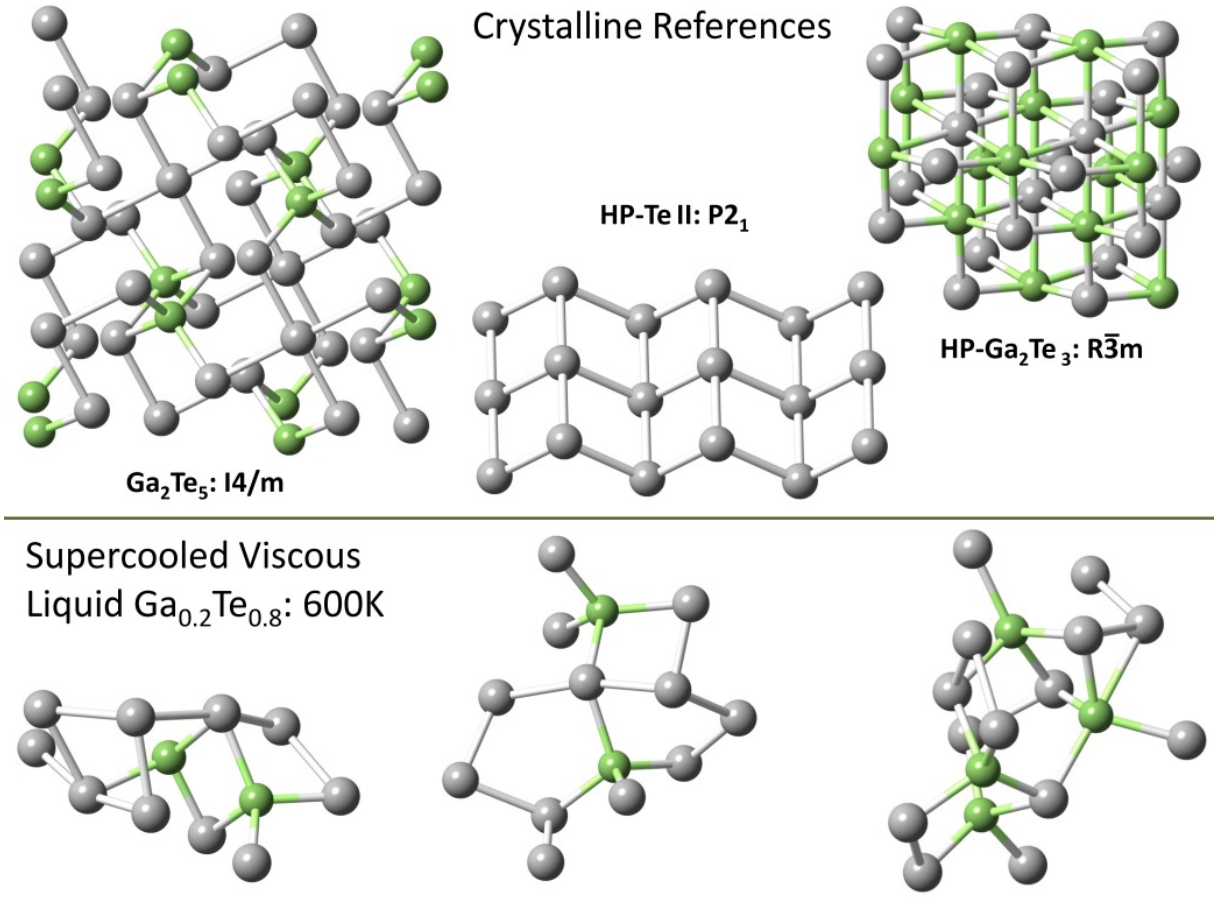

Figure S7. Structural references: tetragonal Ga_2Te_5, space group $I4/m$,[S2,S3] monoclinic HP-Te II, $P2_1$,[S6] and rhombohedral HP-Ga_2Te_3, $R\bar{3}m$,[S5] and HP-motifs in supercooled viscous $Ga_{0.2}Te_{0.8}$ at 600 K (FPMD, this work).

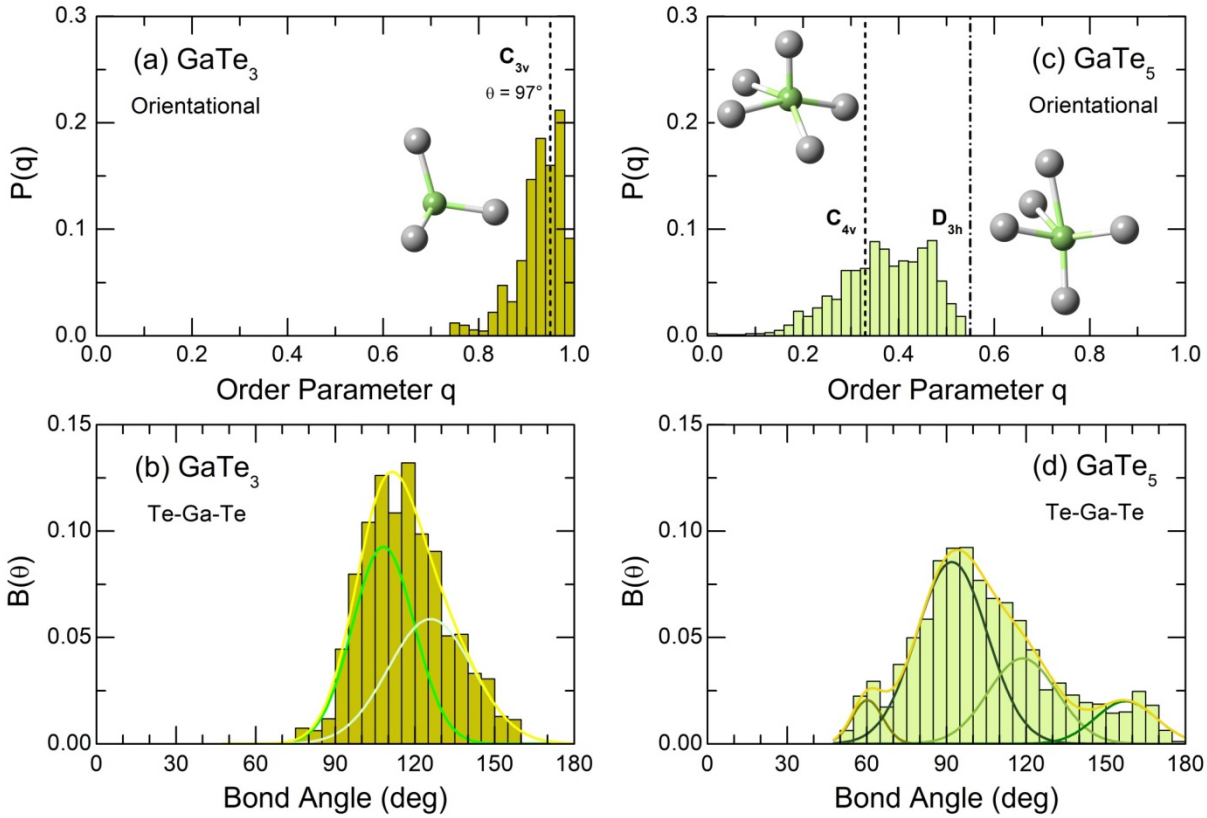

Figure S8. Orientational order parameter q for (a) $GaTe_3$ and (b) $GaTe_5$ entities in liquid $Ga_{0.2}Te_{0.8}$, (b,d) corresponding $B(\theta)$ distributions for Te-Ga-Te bond angles.

Under- and over-coordinated $GaTe_3$ and $GaTe_5$ units in liquid $Ga_{0.2}Te_{0.8}$ also have variable geometry evidenced by broad $B_{\mathrm{TeGaTe}}(\theta)$ distributions of the Te-Ga-Te bond angles, Figure S5b,d. Following Ref. [S7-S9], we have used the orientational order parameter q

$$q = 1 - \frac{3}{8}\sum_{j=1}^{3}\sum_{k=j+1}^{4}\left(\cos\psi_{jk} + \frac{1}{3}\right)^2$$

to determine basic geometry types of these entities. The $GaTe_3$ units often have a pyramidal geometry shown in the inset of Figure S5a. Regular pyramids of C_{3v} symmetry have different q-values dependent on the Te-Ga-Te angle θ: q = 1 for tetrahedral θ_{T_d} = 109.47°, q = ⅞ for octahedral $\theta_{O_h}(2) = \pi/2$, and finally going to q = 0 at $\theta \cong 52.45°$. In addition, flat $GaTe_3$ of D_{3h} symmetry has $q \cong 0.97$, and a T-shaped planar unit of C_{2v} geometry with $\theta_{O_h}(1) = \pi$ and $\theta_{O_h}(2) = \pi/2$ reveals q = ¾. The $P(q)$ probability distribution for $GaTe_3$ appears to be asymmetric and approximately peaked at q = 0.95, corresponding to the C_{3v}-entities with $\theta \cong 97°$. The population of flat and defect tetrahedral $GaTe_3$ species seems to be superior to that of defect octahedral moieties of both pyramidal and planar geometry.

The five-fold coordinated gallium species mostly have a defect octahedral shape, the inset on the left in Figure S5b. A regular square pyramid of C_{4v} symmetry with $\theta_{O_h}(1)$ and $\theta_{O_h}(2)$ angles is characterized by q = ⅓, which is close to the maximum of a broad $P(q)$ distribution for $GaTe_5$. Possible alternative shapes appear to be a trigonal bipyramidal unit of D_{3h} symmetry having $q \approx 0.55$, and a trigonal prism $GaTe_5$ without one Te NN. The defect regular prism with identical Ga-Te distances has $q \cong 0.28$. The fraction of distorted bipyramids, the inset in Figure S5b, or prisms seems to be small.

Table S1. Optimized Geometry Parameters (Ga-Te, Ga-Ga and Te-Te Interatomic Distances, Te-Ga-Te and Ga-Te-Ga Bond Angles) of Size-Limited Ga-Te[a] Clusters Used in DFT Modeling of Vibrational Properties

Compound Cluster	Ga-Te (Å)	Te-Te (Å)	Ga-Ga (Å)	Te-Ga-Te (deg)	Ga-Te-Ga (deg)	X-X-Y (deg)[b]
$GaTe_4$ [a]	2.66(8)	–	–	108(14)	–	–
CS-Ga_2Te_7 [a]	2.71(20)	2.78	4.08 [c]	108(11)	103.2	94(6)
ES-Ga_2Te_6 [a]	2.67(9)	4.14 [c]	3.39 [c]	107(20)	79(4)	–
ES-Ga_3Te_8 [a]	2.67(5)	4.17 [c]	3.34(1) [c]	108(14)	77.4(4)	–
ETH-Ga_2Te_5 [a]	2.65(9)	–	2.50	107(19)	–	116(5)
Ga_2Te_5[S2,S3]	2.641	3.027	3.424	110(8)	80.1	98.8
Ga_2Te_3[S4]	2.553	4.17 [c]	4.17 [c]	109.47	109.47	–
GaTe[S10]	2.67(2)	4.22(15) [c]	2.43(1)	105(4)	96(4)	113(8)

[a] the terminal hydrogen species in the formula are omitted; [b] X = Ga or Te; Y = Ga or Te; [c] the second-neighbor distance

Table S2. Optimized Geometry Parameters (Te-Te Interatomic Distances and Te-Te-Te Bond Angles) of Tellurium Rings Used in DFT Modeling of Vibrational Properties

Compound / Te_n ring	Te-Te (Å)	Te-Te-Te (deg)
Te_6	2.77(8)	102(3)
$(AgI)_2(Te_6)$[S11]	2.74(2)	99(2)
Te_8	2.76(1)	108(9)
Cs_3Te_{22} (Te_8 rings)[S12]	2.80(3)	100(2)

Supporting References

(S1) Cherin, P.; Unger, P. Two-Dimensional Refinement of the Crystal Structure of Tellurium. *Acta Crystal.* **1967**, *23*, 670–671.

(S2) Julien-Pouzol, M.; Jaulmes, S.; Alapini, F. Tellurure de Gallium. *Acta Crystal. B* **1977**, *33*, 2270–2272.

(S3) Deiseroth, H. J.; Amann, P.; Thurn, H. Die Pentatelluride M_2Te_5 (M = Al, Ga, In): Polymorphie, Strukturbeziehungen und Homogenitätsbereiche. *Z. Anorg. Allg. Chem*. **1996**, *622*, 985–993.

(s4) Guymont, M.; Tomas, A.; Guittard, M. The Structure of Ga_2Te_3. An X-ray and High-Resolution Electron Microscopy Study. *Phil. Mag. A: Phys. Cond. Matter* **1992**, *66*, 133–139.

(S5) Serebryanaya, N. R. The Crystal Structure of Pressure-Induced Phases of In_2Te_3 and Ga_2Te_3. *Powder Diffraction* **1992**, *7*, 99–102.

(S6) Aoki, K.; Shimomura, O.; Minomura, S. Crystal Structure of the High-Pressure Phase of Tellurium. *J. Phys. Soc. Japan* **1980**, *48*, 551–556.

(S7) Caravati, S.; Bernasconi, M.; Kühne, T. D.; Krack, M.; Parrinello, M. Coexistence of Tetrahedral- and Octahedral-like Sites in Amorphous Phase Change Materials. *Appl. Phys. Lett*. **2007**, *91*, 171906.

(S8) Caravati, S.; Bernasconi, M.; Parrinello, M. First-Principles Study of Liquid and Amorphous Sb_2Te_3. *Phys. Rev. B* **2010**, *81*, 014201.

(S9) Bouzid, A.; Massobrio, C.; Boero, M.; Ori, G.; Sykina, K.; Furet, E. Role of the van der Waals Interactions and Impact of the Exchange-Correlation Functional in Determining the Structure of Glassy $GeTe_4$. *Phys. Rev. B* **2015**, *92*, 134208.

(S10) Julien-Pouzol, M.; Jaulmes, S.; Guittard, M.; Alapini, F. Monotellurure de Gallium, GaTe. *Acta Crystal. B* **1979**, *35*, 2848–2851.

(S11) Deiseroth, H. J.; Wagener, M.; Neumann, E. $(AgI)_2Te_6$ and $(AgI)_2Se_6$: New Composite Materials with Cyclic Te_6 and Se_6 Molecules Stabilized in the "Solid Solvent" AgI. *Eur. J. Inorg. Chem*. **2004**, *2004*, 4755–4758.

(S12) W. S. Sheldrick, W. S.; Wachhold, M. Discrete Crown-Shaped Te_8 Rings in Cs_3Te_{22}. *Angew. Chem. Int. Ed*. **1995**, *34*, 450–451.